JOURNAL OF BACTERIOLOGY, Apr. 2011, p. 2042–2045 Vol. 193, No. 8
0021-9193/11/$12.00 doi:10.1128/JB.00790-10

NOTES

Crystal Structure of the Autochaperone Region from the *Shigella flexneri* Autotransporter IcsA[▽]†

Karin Kühnel* and Dagmar Diezmann

Department of Neurobiology, Max Planck Institute for Biophysical Chemistry, 37077 Göttingen, Germany

Received 7 July 2010/Accepted 8 February 2011

The IcsA (intracellular spread gene A) autotransporter from *Shigella flexneri* is a key virulence factor. We identified a stable fragment comprising residues 591 to 758, which corresponds to the autochaperone region of the IcsA passenger domain. We showed that thermal unfolding of the autochaperone region is reversible and determined its crystal structure at 2.0-Å resolution.

IcsA (intracellular spread gene A), also denoted VirG (virulence gene G), is an autotransporter that is encoded on the large virulence plasmid of *Shigella flexneri* (14). Autotransporters are secreted through type Va and type Vc secretion systems of Gram-negative bacteria and are almost always virulence factors (8). IcsA belongs to the AIDA-I-like autotransporter family and has the typical domain structure of a type Va autotransporter, with an N-terminal signal sequence followed by a passenger domain (residues 53 to 758) and a transmembrane β-domain (residues 759 to 1102) (Fig. 1A). The C-terminal parts of passenger domains in type Va but not trimeric type Vc autotransporters have been proposed to function as autochaperones critical for secretion and folding (4, 21, 22). Indeed, the importance of this region for the secretion of the IcsA passenger domain (residues 53 to 758) was shown by linker insertion mutagenesis studies (17). IcsA localizes to the bacterial pole (2, 27). It recruits N-WASP (29) and is essential for the actin-based motility of *Shigella* inside infected cells (1, 7). In addition, IcsA is linked to autophagy since its interaction partner IcsB plays a role in the escape of *S. flexneri* from autophagy (20).

We identified a stable IcsA fragment by performing limited proteolysis experiments (Fig. 1B; see also the supplemental material). The construct used in this study comprises residues 591 to 758 and is abbreviated IcsA-AC. IcsA-AC was expressed with an N-terminal hexahistidine tag in *Escherichia coli* and was purified with a three-step procedure (see the supplemental material for a detailed description).

IcsA-AC crystals were grown by hanging-drop vapor diffusion at 20°C by mixing 1 μl of 8 mg/ml protein with 1 μl of the precipitant 17% polyethylene glycol 4000 (PEG 4000), 10% isopropanol, and 0.1 M citrate at pH 6.0. Mother liquor supplemented with 10% ethylene glycol was used as a cryoprotectant. Selenomethionine-substituted IcsA-AC crystals were grown under similar conditions. Diffraction data were collected at the Swiss Light Source (SLS) beamline X10SA (see Table S1 in the supplemental material), and the structure was determined by selenomethionine single-wavelength anomalous diffraction (SAD) phasing.

The final model contains residues 591 to 740, in addition to six residues from the linker region of the N-terminal His tag (Fig. 1C). The last 18 residues of IcsA-AC are disordered. The structure was refined to final R factor and R_{free} values of 19.7% and 21.9% at 2.0-Å resolution, respectively (see Table S1 in the supplemental material).

IcsA-AC forms two coils of a right-handed parallel β-helix. The cross section is "V" shaped, with a width of 30 Å (Fig. 1C). Each coil consists of three β-strands. The first strand of coil 1 originates from the linker region of the His tag (Fig. 1C). The C-terminal part of IcsA-AC forms a β-sandwich that is capped by the last two antiparallel β-strands, which shield the hydrophobic core from the solvent.

In the crystal lattice, IcsA-AC is arranged as a head-on-head dimer. However, in solution, the protein appears to be monomeric. IcsA-AC elutes in a single peak from a gel filtration column (see Fig. S1 in the supplemental material). The molecular mass calculated from the elution volume is 26 kDa, and the expected molecular mass of a monomer is 20 kDa. The passenger domains of more than 97% of type Va autotransporters are predicted to adopt a β-helical fold (12). One exception is EstA, an esterase from *Pseudomonas aeruginosa*, whose passenger domain has an α-helix and a loop-rich globular fold (30). However, despite the large number of autotransporters occurring in nature, only four β-helical passenger domain structures have been determined so far (5, 6, 10, 23). IcsA-AC resembles the autochaperone regions of pertactin, hemoglobin protease, and immunoglobulin A1 protease, which all adopt a β-sandwich fold (18). In fact, a DALI search (9) revealed that IcsA-AC is most similar to pertactin. IcsA-AC and pertactin (residues 436 to 571) superimpose with a root mean square deviation (RMSD) of 1.9 Å and share 20% sequence identity for these regions, whereas the sequence iden-

* Corresponding author. Mailing address: Department of Neurobiology, Max Planck Institute for Biophysical Chemistry, Am Faßberg 11, 37077 Göttingen, Germany. Phone: 49 551 201 1795. Fax: 49 551 201 1499. E-mail: kkuehne@gwdg.de.

† Supplemental material for this article may be found at http://jb.asm.org/.

▽ Published ahead of print on 18 February 2011.

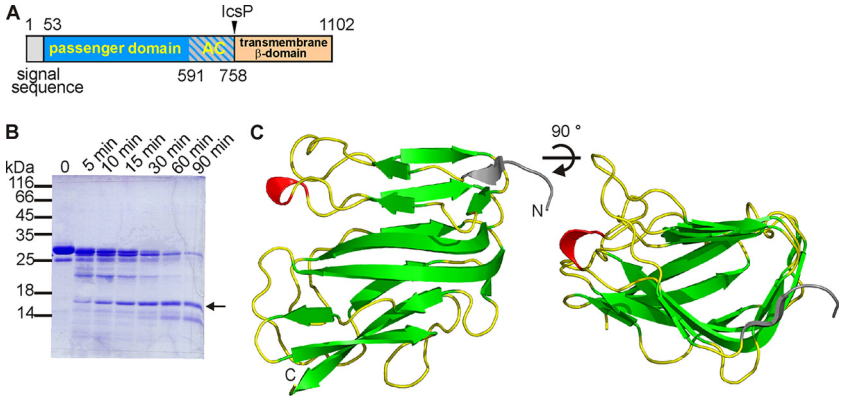

FIG. 1. Identification of the IcsA-AC fragment and its structure. (A) Domain structure of IcsA. The construct used in this study is marked. The protease IcsP cleaves the passenger domain from the transmembrane domain after translocation (28). (B) A stable IcsA fragment, marked with an arrow, was formed during limited proteolysis experiments with IcsA (residues 489 to 752) and proteinase K. (C) Side and top views of IcsA-AC. The residues of the N-terminal linker region are colored in gray, β-strands are labeled in green, and a short α-helical stretch (residues 628 to 630) is marked in red. The figures were prepared with PyMOL (http://www.pymol.org) (DeLano Scientific LLC, San Carlos, CA). N, N terminus; C, C terminus.

tity for the complete passenger domains of IcsA (residues 53 to 758) and pertactin (residues 35 to 711) is only 10%.

In general, the C-terminal regions of passenger domains show a low level of sequence conservation among different autotransporters, indicating a conserved role during secretion (22). This region has been assigned as a domain in the ProDom database (3), entry PD002475 (22), and is found in 113 autotransporters, including IcsA. To identify further close homologues, we performed a FASTA search (16) of the UniProt database with the IcsA-AC sequence. The IcsA homologues of the other three *Shigella* serogroups are highly conserved, with 99 to 100% sequence identities. The *E. coli* adhesin AIDA-I (residues 796 to 959) shares 35% sequence identity with IcsA-AC. In addition, a number of predicted autotransporters were found. Sequence alignment was performed with T-Coffee (19), and the aligned sequences were further analyzed with the AMAS server (15) (see Fig. S2 in the supplemental material). For visualization, the conserved residues were colored according to their degree of conservation (Fig. 2A and B). The C-terminal part of IcsA-AC is more conserved than the N-terminal part of the molecule. Near the C terminus, there is also a conserved surface patch, which is mainly nonpolar, but the basic Arg710 is strongly conserved (Fig. 2B and C). We speculate that this region could be of functional importance and might be involved in protein-protein interactions during translocation across the outer membrane.

Limited proteolysis experiments of chemically denatured pertactin (12) and plasmid-encoded toxin from *E. coli* (26) showed the presence of a stable core at the C termini of these passenger domains. To characterize the stability of IcsA-AC, we used far-UV circular dichroism (CD) spectroscopy. A thermal unfolding curve was recorded at between 20 and 90°C (Fig. 3A). IcsA-AC is stable, with a thermal transition midpoint of 46°C, and unfolding occurs in a single transition. At 60°C, IcsA-AC is unfolded, and the spectrum has a minimum at 203 nm, characteristic for an unfolded protein (Fig. 3B), whereas at 20°C, the spectrum shows a local minimum at 216 nm, which is a typical feature for a folded β-strand-rich protein (13).

The autochaperone region first reaches the outer membrane surface during secretion, and it has been suggested that by adopting its native conformation, the autochaperone region could serve as a template for the folding of the complete

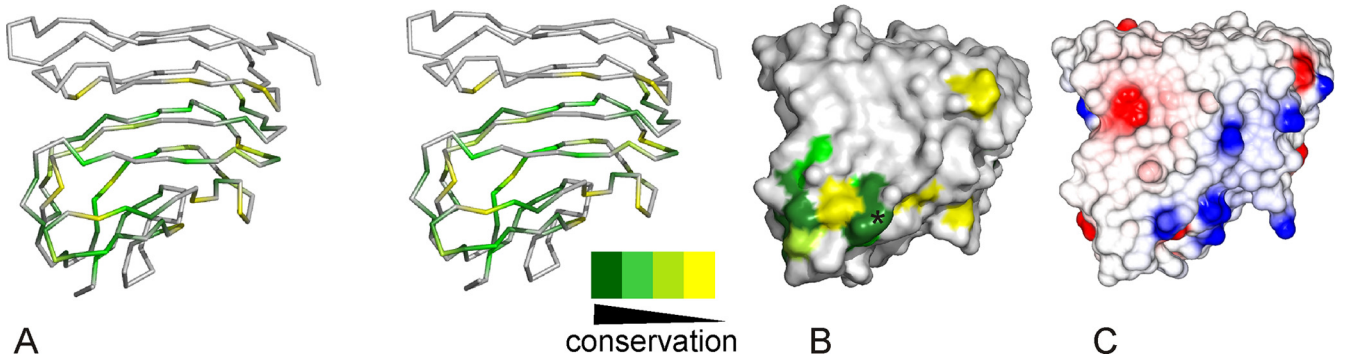

FIG. 2. Sequence conservation of IcsA-AC. (A) Stereoview of the IcsA-AC backbone, with the residues color coded according to their degree of conservation. (B) Surface presentation showing the level of conservation, colored as described in the legend to panel A. The conserved residue Arg710 is marked with an asterisk. (C) Electrostatic surface representation of IcsA-AC. This figure was generated with the program CCP4mg (25). The molecules depicted in Fig. 3 are shown in the same orientation.

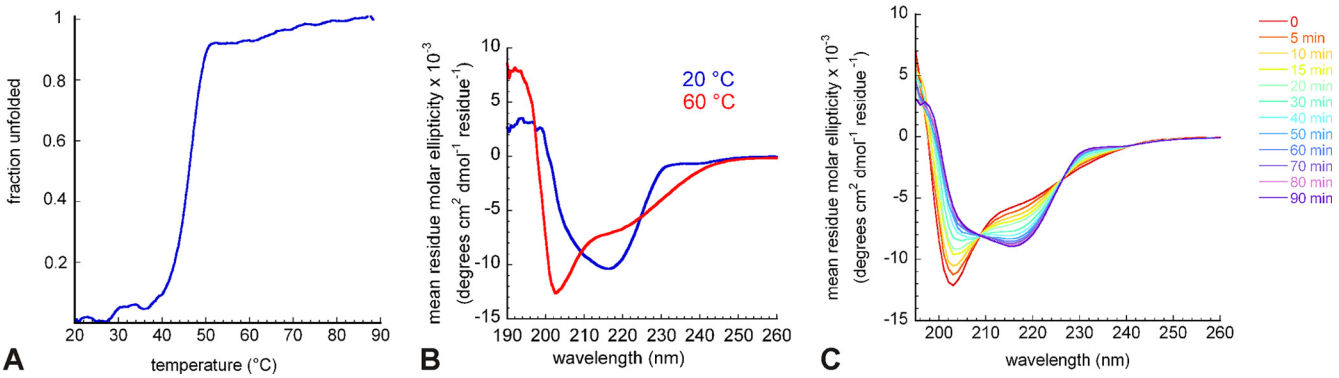

FIG. 3. Stability and reversible thermal unfolding of IcsA-AC. (A) The IcsA-AC melting curve was recorded by measuring the ellipticity at 216 nm. All CD measurements were done in 0.3 M NaF and 30 mM NaH_2PO_4 at pH 7.5. (B) Far-UV CD spectra of IcsA-AC were measured at 20°C and at 60°C. (C) IcsA-AC was first denatured by heating it to 60°C for 20 min. The probe was then cooled to 20°C, and spectra were recorded continuously at a constant temperature.

passenger domain (11, 12). To do so, the autochaperone region should be capable of self-contained refolding after denaturation of the protein. We tested that by first unfolding IcsA-AC by heating it to 60°C. The sample was then cooled to 20°C, and spectra were continuously measured every 5 min at this temperature. The protein was completely refolded after approximately 1 h (Fig. 3C). After this period, the spectra showed minima at 216 nm, resembling those of native IcsA-AC recorded at 20°C (Fig. 3B). Refolding occurring at 37°C was as fast as that occurring at 20°C (see Fig. S3A in the supplemental material). However, the CD spectra of the refolded protein display a broader trough in the region of 204 to 216 nm than that displayed by the spectra of the native protein (Fig. 3B). Since IcsA-AC has no catalytic activity or known binding partner, we probed the properties of the refolded protein with a proteinase K digestion assay and by analytical gel filtration. The refolded sample eluted from the gel filtration column in the same way as the native protein (see Fig. S3B in the supplemental material), which excludes the formation of β-amyloidic aggregates after thermal denaturation.

In a proteolytic digestion assay, the protein was first denatured by heating it for 30 min at 60°C and then incubating it at 20°C (see Fig. S3C in the supplemental material). Samples were taken at regular intervals and treated with proteinase K. The heat-denatured sample was entirely degraded by the protease; however, after incubation at 20°C, the formation of a 15-kDa fragment was observed, and the maximum intensity of this band was reached after 60 to 90 min. This stable fragment also formed when a nonheated control sample kept at 20°C was digested. The refolded protein can also be crystallized under conditions similar to those used for the untreated native protein (see Fig. S3D in the supplemental material). In all these experiments, refolded IcsA-AC behaved the same as the native untreated protein. These results provide strong evidence that unfolded IcsA-AC adopts its native structure without the need of an extra chaperone, albeit slowly. Recently, it was shown that the folding of the C-terminal part of the EspP passenger domain drives the secretion of the passenger domain, highlighting the importance of the autochaperone regions of type Va autotransporters (24). The studies presented here need to be extended to the full-length passenger domain to obtain further structural insights into this key virulence factor of *S. flexneri*.

Protein structure accession number. The atomic coordinates and structure factors were deposited in the Protein Data Bank under accession number 3ML3.

Diffraction data were collected at beamline X10SA (Swiss Light Source, Paul Scherrer Institute, Villigen, Switzerland), and we thank the beamline staff for assistance during data collection. We further thank R. Lührmann, M. Wahl, and V. Pena for access to the local X-ray infrastructure and A. Zychlinsky for kindly providing the *S. flexneri* pWR100 plasmid. We are very grateful to R. Jahn for valuable discussions and his generous support.

REFERENCES

1. **Bernardini, M. L., J. Mounier, H. d'Hauteville, M. Coquis-Rondon, and P. J. Sansonetti.** 1989. Identification of icsA, a plasmid locus of Shigella flexneri that governs bacterial intra- and intercellular spread through interaction with F-actin. Proc. Natl. Acad. Sci. U. S. A. **86:**3867–3871.
2. **Charles, M., M. Perez, J. H. Kobil, and M. B. Goldberg.** 2001. Polar targeting of Shigella virulence factor IcsA in Enterobacteriacae and Vibrio. Proc. Natl. Acad. Sci. U. S. A. **98:**9871–9876.
3. **Corpet, F., F. Servant, J. Gouzy, and D. Kahn.** 2000. ProDom and ProDom-CG: tools for protein domain analysis and whole genome comparisons. Nucleic Acids Res. **28:**267–269.
4. **Dutta, P. R., B. Q. Sui, and J. P. Nataro.** 2003. Structure-function analysis of the enteroaggregative Escherichia coli plasmid-encoded toxin autotransporter using scanning linker mutagenesis. J. Biol. Chem. **278:**39912–39920.
5. **Emsley, P., I. G. Charles, N. F. Fairweather, and N. W. Isaacs.** 1996. Structure of Bordetella pertussis virulence factor P.69 pertactin. Nature **381:**90–92.
6. **Gangwer, K. A., et al.** 2007. Crystal structure of the Helicobacter pylori vacuolating toxin p55 domain. Proc. Natl. Acad. Sci. U. S. A. **104:**16293–16298.
7. **Goldberg, M. B., and J. A. Theriot.** 1995. Shigella flexneri surface protein IcsA is sufficient to direct actin-based motility. Proc. Natl. Acad. Sci. U. S. A. **92:**6572–6576.
8. **Henderson, I. R., F. Navarro-Garcia, M. Desvaux, R. C. Fernandez, and D. Ala'Aldeen.** 2004. Type V protein secretion pathway: the autotransporter story. Microbiol. Mol. Biol. Rev. **68:**692–744.
9. **Holm, L., and C. Sander.** 1993. Protein structure comparison by alignment of distance matrices. J. Mol. Biol. **233:**123–138.
10. **Johnson, T. A., J. Qiu, A. G. Plaut, and T. Holyoak.** 2009. Active-site gating regulates substrate selectivity in a chymotrypsin-like serine protease the structure of haemophilus influenzae immunoglobulin A1 protease. J. Mol. Biol. **389:**559–574.
11. **Junker, M., R. N. Besingi, and P. L. Clark.** 2009. Vectorial transport and folding of an autotransporter virulence protein during outer membrane secretion. Mol. Microbiol. **71:**1323–1332.
12. **Junker, M., et al.** 2006. Pertactin beta-helix folding mechanism suggests common themes for the secretion and folding of autotransporter proteins. Proc. Natl. Acad. Sci. U. S. A. **103:**4918–4923.

13. **Kelly, S. M., T. J. Jess, and N. C. Price.** 2005. How to study proteins by circular dichroism. Biochim. Biophys. Acta **1751:**119–139.
14. **Lett, M. C., et al.** 1989. virG, a plasmid-coded virulence gene of Shigella flexneri: identification of the virG protein and determination of the complete coding sequence. J. Bacteriol. **171:**353–359.
15. **Livingstone, C. D., and G. J. Barton.** 1993. Protein sequence alignments: a strategy for the hierarchical analysis of residue conservation. Comput. Appl. Biosci. **9:**745–756.
16. **Mackey, A. J., T. A. Haystead, and W. R. Pearson.** 2002. Getting more from less: algorithms for rapid protein identification with multiple short peptide sequences. Mol. Cell. Proteomics **1:**139–147.
17. **May, K. L., and R. Morona.** 2008. Mutagenesis of the Shigella flexneri autotransporter IcsA reveals novel functional regions involved in IcsA biogenesis and recruitment of host neural Wiscott-Aldrich syndrome protein. J. Bacteriol. **190:**4666–4676.
18. **Nishimura, K., N. Tajima, Y. H. Yoon, S. Y. Park, and J. R. Tame.** 2010. Autotransporter passenger proteins: virulence factors with common structural themes. J. Mol. Med. **88:**451–458.
19. **Notredame, C., D. G. Higgins, and J. Heringa.** 2000. T-Coffee: a novel method for fast and accurate multiple sequence alignment. J. Mol. Biol. **302:**205–217.
20. **Ogawa, M., et al.** 2005. Escape of intracellular Shigella from autophagy. Science **307:**727–731.
21. **Ohnishi, Y., M. Nishiyama, S. Horinouchi, and T. Beppu.** 1994. Involvement of the COOH-terminal pro-sequence of Serratia marcescens serine protease in the folding of the mature enzyme. J. Biol. Chem. **269:**32800–32806.
22. **Oliver, D. C., G. Huang, E. Nodel, S. Pleasance, and R. C. Fernandez.** 2003. A conserved region within the Bordetella pertussis autotransporter BrkA is necessary for folding of its passenger domain. Mol. Microbiol. **47:**1367–1383.
23. **Otto, B. R., et al.** 2005. Crystal structure of hemoglobin protease, a heme binding autotransporter protein from pathogenic Escherichia coli. J. Biol. Chem. **280:**17339–17345.
24. **Peterson, J. H., P. Tian, R. Ieva, N. Dautin, and H. D. Bernstein.** 2010. Secretion of a bacterial virulence factor is driven by the folding of a C-terminal segment. Proc. Natl. Acad. Sci. U. S. A. **107:**17739–17744.
25. **Potterton, L., et al.** 2004. Developments in the CCP4 molecular-graphics project. Acta Crystallogr. D Biol. Crystallogr. **60:**2288–2294.
26. **Renn, J. P., and P. L. Clark.** 2008. A conserved stable core structure in the passenger domain beta-helix of autotransporter virulence proteins. Biopolymers **89:**420–427.
27. **Robbins, J. R., et al.** 2001. The making of a gradient: IcsA (VirG) polarity in Shigella flexneri. Mol. Microbiol. **41:**861–872.
28. **Shere, K. D., S. Sallustio, A. Manessis, T. G. D'Aversa, and M. B. Goldberg.** 1997. Disruption of IcsP, the major Shigella protease that cleaves IcsA, accelerates actin-based motility. Mol. Microbiol. **25:**451–462.
29. **Suzuki, T., H. Miki, T. Takenawa, and C. Sasakawa.** 1998. Neural Wiskott-Aldrich syndrome protein is implicated in the actin-based motility of Shigella flexneri. EMBO J. **17:**2767–2776.
30. **van den Berg, B.** 2010. Crystal structure of a full-length autotransporter. J. Mol. Biol. **396:**627–633.